

Excited-State Intramolecular Proton Transfer in Five-Membered Hydrogen-Bonding Systems: 2-Pyridyl Pyrazoles

Wei-Shan Yu,[†] Chung-Chih Cheng,[†] Yi-Ming Cheng,[†] Pei-Chi Wu,[‡] Yi-Hwa Song,[‡] Yun Chi,^{*,‡} and Pi-Tai Chou^{*,†}

Department of Chemistry, National Taiwan University, 106, Taipei, Taiwan R.O.C., and Department of Chemistry, National Tsing Hua University, 300, Hsinchu, Taiwan R.O.C.

Received March 31, 2003; E-mail: chop@ntu.edu.tw

Since the seminal studies on the excited-state intramolecular proton transfer (ESIPT) reaction in salicylic derivatives,¹ numerous ESIPT molecules have been discovered and investigated to shed light on their corresponding spectroscopy and dynamics.² Most ESIPT molecules possess six-membered ring types of a strong intramolecular hydrogen bond between O–H (or N–H) and C=O (or pyridinic nitrogen) groups, in which the intramolecular proton transfer in the $^1\pi\pi^*$ state³ commonly reveals a negligible barrier in nonpolar solvents and may proceed during the period of low-frequency vibrational motions associated with the hydrogen bond.^{4–7}

From the fundamental viewpoint, searching for the ESIPT reaction with a finite, well-defined barrier is of great importance to gain detailed insights into the reaction potential energy surface. To achieve this goal, conjugated pyrrole-pyridine systems such as 1-*H*-pyrrolo[3, 2-*h*]quinolines⁸ possessing an N–H···N type of five-membered hydrogen bond have received much attention. Under similar proton donor/acceptor strengths, the intramolecular hydrogen-bonding (HB) strength is empirically on the order of $6 > 5 \gg 4$ four-membered systems due to the steric and orientation effects. Unlike the O–H site that has certain rotational degrees of freedom, the orientation effect of the pyrrolic N–H site being restricted toward a specific direction becomes more critical for the HB formation. Furthermore, the photoacidity of the pyrrolic hydrogen is in general weaker than that of the phenolic hydrogen. As a result, ESIPT in five-membered HB pyrrole–pyridine systems may be associated with an appreciably large barrier. Unfortunately, to our knowledge, none of the five-membered N–H···H HB systems have yet been reported to exhibit intrinsic ESIPT. Instead, similar to the four-membered proton donor/acceptor systems such as the 7-azaindoles,⁹ this class of molecules is well-known to undergo a guest molecule (including the protic solvents)-catalyzed excited-state proton-transfer reaction.⁸

In this study, we have alternatively designed and synthesized the conjugated 2-pyridyl pyrazole systems where the N(1)–H acidity is enhanced via the electron-withdrawing property of the proximal nitrogen atom (N(2), see Scheme 1) in the pyrazole ring. Scheme 1 shows the molecular drawings of 5-(2-pyridyl) 1-*H*-pyrazoles **1a–d**, possessing various substituents at the –3 position.¹⁰ Both X-ray structural analyses and molecular modeling indicate that the N(1)–H···N(1') HB isomer is the predominant species for **1a–d** in the ground state (see Supporting Information).

Prototypical absorption and emission spectra of **1a** in thoroughly dry cyclohexane are depicted in Figure 1. Upon $S_0 \rightarrow S_1$ ($\pi\pi^*$) excitation ($\lambda_{\text{max}} \approx 290$ nm, $\epsilon_{290} \approx 1.2 \times 10^4$ M⁻¹ cm⁻¹), dual fluorescence was observed maximized at 320 nm (the F₁ band) and 585 nm (the F₂ band). The excitation spectra monitored at F₁ and

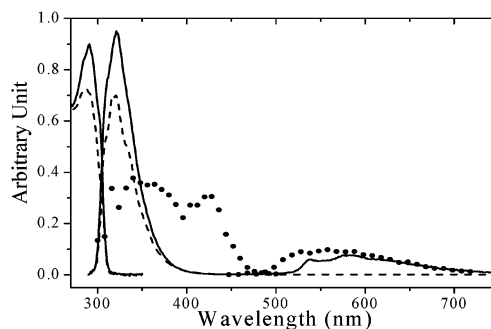
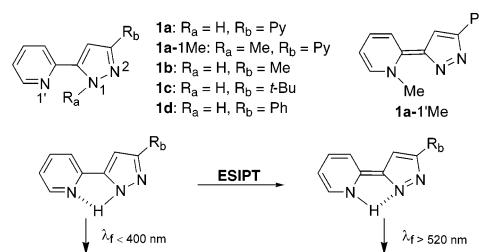


Figure 1. The absorption and emission spectra of (a) **1a** (—), 1.0×10^{-5} M, (b) **1a-1Me** (---) and (c) **1a-1'Me** (···) in cyclohexane. The excitation wavelength is 280 nm.

Scheme 1. Structures and Proposed ESIPT Mechanism for the Studied Systems



F_2 bands are identical, and are effectively the same as the $S_0 \rightarrow S_1$ absorption spectral feature, indicating that both emission bands originate from the same ground-state precursor. In a comparative study, **1a-1Me** (see Scheme 1), which serves as a nonproton-transfer model, exhibits a normal Stokes shifted emission maximum at ~ 318 nm. Conversely, the proton-transfer tautomer analogue **1a-1'Me** reveals a single fluorescence maximum at ~ 570 nm of which the spectral feature is similar to that of the F_2 band. We thus conclude that ESIPT takes place in **1a**, resulting in an anomalously large Stokes-shifted ($> 10\,000$ cm⁻¹) proton-transfer tautomer emission. Similar dual emissions were resolved in **1b–d**, of which the corresponding photophysical properties are listed in Table 1.

In contrast to the exclusive tautomer emission resulting from the ultrafast proton-transfer reaction for most ESIPT molecules,⁴ the appearance of dual emissions in **1a–d** in which the normal fluorescence is prevailing is remarkable. It implies the existence of an appreciably high barrier associated with ESIPT so that the decay dynamics of the locally excited $S_1 \rightarrow S_0$ relaxation is competitive with the rate of proton transfer. Further insight into the reaction mechanism was gained from the dynamic studies. Single-exponential decay kinetics were resolved for the F_1 band of **1a**, and a lifetime was fitted to be ~ 85 ps ($\chi^2 = 1.02$) at 298 K, while the F_2 band is apparently composed of rise and decay compo-

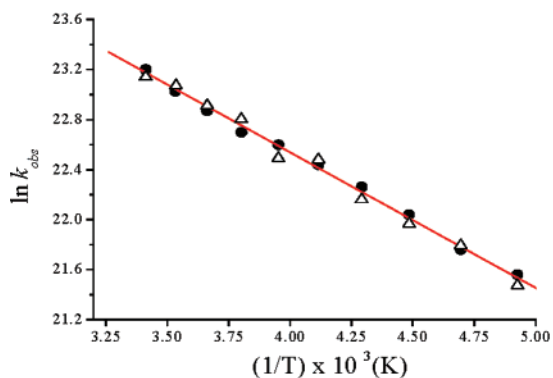
[†] Department of Chemistry, National Taiwan University, 106, Taipei, Taiwan R.O.C.

[‡] Department of Chemistry, National Tsing Hua University, 300, Hsinchu, Taiwan R.O.C.

Table 1. Photophysical Parameters of **1a–d** Measured in Cyclohexane at 298 K

	$\lambda_{\max}^{F_1} (\Phi^a)$	$\lambda_{\max}^{F_2} (\Phi^a)$	F_1^b	F_2^b	ΔE^d
1a	320 (19)	585(1.5)	85	80 (−0.071) ^c 275 (0.065)	2.03
1b	320 (21)	577(0.5)	115	120 (−0.017) 242 (0.021)	2.22
1c	320 (25)	577(0.2)	125	130 (−0.042) 213 (0.035)	2.62
1d	322 (9)	590(0.3)	74	76 (−0.070) 175 (0.061)	1.76

^a $\Phi \times 10^3$. ^b Picoseconds. ^c Numbers in the parenthesis are preexponential factors of the fitting eq $F(t) = a_1 e^{-k_1 t} + a_2 e^{-k_2 t}$. ^d ΔE (in kcal/mol) measured in methylcyclohexane. λ in nm.

**Figure 2.** The plot for $\ln k_{\text{obs}}$ versus the reciprocal of temperatures in methylcyclohexane: **1a-h** (●) and **1a-d** (△) (monitored at the F_1 band).

nents that were fitted to be 80 and 275 ps, respectively ($\chi^2 = 1.01$). The rise time of the F_2 band, within experimental error, is identical with the decay time of the F_1 band, further supporting the precursor–successor type of reaction mechanism. ESIPT dynamics were also obtained for **1b–d** at 298 K and the results are listed in Table 1.

The rate constants of 70–130 ps^{−1} measured for **1a–d** are ~2 orders of magnitude smaller than that reported for typical ESIPT molecules in nonpolar solvents.⁴ Slower proton-transfer reaction may be in some way associated with its rather weak hydrogen-bonding strength, and hence a long HB distance. Thus, one might initially suspect that this is simply due to a larger barrier along the reaction coordinate with only the proton motion involved. To test this possibility, the ESIPT rates in deuterated (N(1)–D) versions of **1a–d** were investigated. If only proton motion is involved in the reaction coordinate, a large deuterium isotope effect would be predicted. However, as shown in Figure 2, within experimental errors, our results reveal a negligible isotope effect.

Accordingly, more than proton motion must be involved in the reaction coordinate. Molecular modeling of **1a** renders a relatively long N(1)H...N(1') HB distance of ~2.49 Å with an N–H...N angle of ~93°. These results, in combination with the restricted orientation of the pyrazole N–H bond, lead us to propose that the reaction coordinate does not couple directly with the N–H stretching mode. Rather, it involves other skeletal motions such as in-plane bending modes, which change the relative position of atoms associated with the hydrogen bond, and hence channel into the proton-transfer process. In this case, the resulting effective tunneling mass should be greatly increased so that the deuteration of amino proton results in only a very small fractional increase in the

tunneling mass. As a result, a negligible H/D isotope effect would be observed. We further carried out a series of temperature-dependent studies regarding reaction dynamics. As shown in Figure 2, the reaction rate for **1a** monitored by the decay dynamics of the F_1 band or equivalently the rise dynamics of the F_2 band revealed significant temperature dependence in the range of 298–203 K.¹² The logarithm plot for the ESIPT rate versus $1/T$ is sufficiently linear, from which a nearly deuterium isotope independent barrier ($\Delta E \approx 2.03$ kcal/mol) and frequency factor ($\sim 3.8 \times 10^{11}$ s^{−1}) were deduced. Negligible N–D isotope ESIPT dynamics were also observed for **1b–d**, and their corresponding ΔE are listed in Table 1. Upon increasing the electron-withdrawing ability in R_b (see Scheme 1) the acidity of the N(1)–H proton should increase, and hence faster ESIPT dynamics is expected. In contrast, Table 1 shows a lack of correlation between ΔE and donating/accepting properties of R_b , indirectly supporting the skeletal reorganization facilitating ESIPT process. Further support was given by a similar Arrhenius plot for **1a** in dry CH₃CN, and ΔE was deduced to be ~2.90 kcal/mol, consistent with that obtained in methylcyclohexane.

In conclusion, the results demonstrate a novel and unique system among ESIPT molecules where the intrinsic proton transfer is associated with a substantial energy barrier. The nature of the reaction potential surface in **1a–d** may be described by certain skeletal reorganization and hence is of a great theoretical challenge. This, in combination with the structural simplicity and diversity, makes the 5-(2-pyridyl)-1-*H*-pyrazole system an ideal model for probing ESIPT dynamics, which are believed to bring up a broad spectrum of interests in the proton-transfer field.

Supporting Information Available: Detailed experimental procedures, absorption, emission, time-resolved, and X-ray studies (PDF/CIF). This material is available free of charge via the Internet at <http://pubs.acs.org>.

References

- (1) Weller, A. Z. *Electrochem.* **1956**, *60*, 1144.
- (2) For recent reviews, see: (a) Scheiner, S. *J. Phys. Chem. A* **2000**, *104*, 5898. (b) Waluk, J. Conformational aspects of intra- and intermolecular excited state proton transfer. In *Conformational Analysis of Molecules in Excited States*; Waluk, J., Ed.; Wiley-VCH: 2000. (c) Chou, P. T. *J. Chin. Chem. Soc.* **2001**, *48*, 651.
- (3) The prohibition of ESIPT in the $n\pi^*$ state has been reported in several ESIPT molecules. For example, see ref 2a.
- (4) For example, see: (a) Chudoba, C.; Riedle, E.; Pfeiffer, M.; Elsaesser, T. *Chem. Phys. Lett.* **1996**, *263*, 622. (b) Lochbrunner, S.; Wurzer, A. J.; Riedle, E. *J. Chem. Phys.* **2000**, *112*, 10699. (c) Chou, P. T.; Chen, Y. C.; Yu, W. S.; Chou, Y. H.; Wei, C. Y.; Cheng, Y. M. *J. Phys. Chem. A* **2001**, *105*, 1731. (d) Ameer-Beg, S.; Ormson, S. M.; Brown, R. G.; Matousek, P.; Towrie, M.; Nibbering, E. T. J.; Foggi, P.; Neuwahl, F. V. *R. J. Phys. Chem. A* **2001**, *105*, 3709. (e) Stock, K.; Bizjak, T.; Lochbrunner, S. *Chem. Phys. Lett.* **2002**, *354*, 409.
- (5) One exceptional case is 3-hydroxyflavones possessing a five-membered ring =O...H–O hydrogen bond. Ultrafast ESIPT was reported for 3-hydroxyflavone (3HF) in nonpolar solvents.^{4d} Barrierless excited-state proton transfer in 3HF was also reported through the cyclic hydrogen bond with protic solvents such as methanol.⁶
- (6) Schwartz, B. J.; Peteanu, L. A.; Harris, C. B. *J. Phys. Chem.* **1992**, *96*, 3591.
- (7) The ESIPT from phenol O–H to a β -carbon atom is not included in this category, see: Lukeman, M.; Wan, P. *J. Am. Chem. Soc.* **2002**, *124*, 9458.
- (8) For recent examples, see: (a) Kyrchenko, A.; Herbich, J.; Izydorzak, M.; Wu, F.; Thummel, R. P.; Waluk, J. *J. Am. Chem. Soc.* **1999**, *121*, 11179. (b) Herbich, J.; Kijak, M.; Zielińska, A.; Thummel, R. P.; Waluk, J. *J. Phys. Chem. A* **2002**, *106*, 2158.
- (9) Taylor, C. A.; El-Bayoumi, A. M.; Kasha, M. *Proc. Natl. Acad. Sci. U.S.A.* **1969**, *65*, 253. Also, see refs 2b and 2c for recent reviews.
- (10) See Supporting Information for detailed syntheses and characterization.
- (11) The calculation was based on the HF/6-31G(d',p') level. X-ray data were not applied here due to the dimeric structure in a single crystal.
- (12) Further decreasing temperatures resulted in microcrystals interferences.

JA035382Y